J. Indian Inst. Sci., July–Aug. 2005, **85**, 223–234

Laser ablation-inductively coupled plasma mass spectrometry for 2D mapping of trace elements in soft tissues

N. CHANDRA SEKARAN*
University of Aberdeen, Department of Chemistry, Old Aberdeen, Meston Walk, AB24 3UD, Scotland, UK.
email: Natarajan@green.gifu-u.ac.jp. Tel: 0081-58-293-2072; Fax: 0081-58-293-2079.

Received on February 2, 2005.

Abstract

Metals are not homogeneously distributed in organ tissues. Although most mapping techniques, such as histologic staining methods, have been developed for element imaging on a subcellular level, many suffer from either low precision or poor detection limits. Therefore, small variations in elemental distribution cannot be identified. We have developed a method for two-dimensional mapping of trace elements to identify the influence of metabolic zonation by the liver on trace element distribution.

Keywords: LA-ICP-MS, mapping, copper zonation, soft tissues, CRM pig liver paste (LG7112).

1. Introduction

Laser ablation has been used in the determination of trace elements in many nonbiological solid samples like glass [1], geological materials [2], metal sheets [3], polymers [4], and even ice cores [5]. Although there have been a few studies on biological samples, all of them were hard tissues like tree rings [6–9], tree barks [10], teeth [11–12], leaves [13] and shells from bivalves [14–17] and very limited information is available on the applicability of a laser ablation system for fresh soft tissues like liver or brain.

In biological and clinical applications it is often desirable to have knowledge of the distribution of a trace element in a soft tissue. Traditionally, pathologists have used staining methods for different elements of interest. These methods have disadvantages: they are often not sensitive enough to detect trace and ultratrace concentrations of elements, or the chemicals used for staining introduce impurities [18]. Although these methods are element specific, this is a disadvantage if more than one element has to be mapped in the tissue. In addition, some of the chemical reactions are very metal species specific. For example, complexing agents must compete with cysteine-rich proteins (metallothioneins) to bind the metal. Thus, staining methods such as the rhodamine method for copper can identify free copper but not the copper bound in copper proteins [19]. Other methods, such as scanning nuclear microprobes [18], microPIXE [20], secondary ion mass spectrometry [21, 22], laser microprobe mass analysis [23], energy-dispersive X-ray analysis [24–26], and electron probe X-ray microanalysis [27] suffer from either low precision or poor detection limits.

*Preset address: River Basin Research Center, 1-1 Yanagido, GIFU University, Japan.

Laser microprobe mass analysis, however, is an ideal technique for the determination of trace element distribution in biological samples. It is rather a sensitive tool, with detection limits in the upper ppm range (1–100 μg/g). However, because the ionization of elements is strongly dependent on the matrix and therefore rather difficult to calibrate, this technique can be considered only as a qualitative method. Furthermore, the thin sections should not be thicker than 2 μm, which makes sample preparation rather difficult.

Laser ablation (LA) [20] methods have been used extensively for mapping of elements and organic compounds in soft tissue. Recent developments in matrix-assisted laser desorption–ionization time-of-flight mass spectrometry allow a spatial resolution of 30 *m*m for the direct mapping of compounds in the mass range between 1 and 50 kDa in tissue sections [21, 28]. However, when an LA system is coupled to an inductively coupled plasma mass spectrometer (ICP-MS), the ablated material is fully ionized in the argon plasma and the elements are detected by an element-specific detector [29].

The present study envisages the applicability of laser ablation towards 2D mapping of trace elements in lamb liver (New Zealand) section. Trace element availability in the bulk tissue state the total concentration of the element in the tissue concerned, but is difficult to localize in the tissues. Therefore, this technique was adopted to explore the possibility of determining the elemental distribution and to map its specific localization and to quantify it using certified reference material (CRM) pig liver paste (LG-7112).

2. Aims and objectives

1. To show precision and accuracy of LA-ICP-MS using cryogenic ablation chamber.
2. To show the potential of elemental mapping using (a) homogenous CRM pig liver (LG-7112) (b) heterogeneous liver section (30-*m*m cryomicrotome section).

3. Material and methods

3.1. *Instrumental set-up*

A commercially available UV Nd-YAG laser with an excitation wavelength of 266 nm (CETAC LSX-200 Plus and DigiLaz operating software) which was coupled to an ICP-TOF-MS (Renaissance, LECO) was used. However, a cryogenically cooled ablation cell of similar size (volume: 60 ml) replaced the commercial ablation chamber. A temperature sensor and a copper-cooling coil were incorporated at the bottom of the cell. The temperature sensor was connected to a temperature controller, which controlled the liquid nitrogen supply stored in a Dewar (volume: 1.35 l) to the ablation chamber by a solenoid valve. A schematic of the ablation cell can be seen in Figs 1 and 2. The temperature can be controlled easily from –20 to –100°C with a variance of ± 3°C within the ablation cell. It should be noted that the sensor does not measure the temperature of the sample but only of the ablation cell surface.

The ICP-MS is tuned on *m*/*z* 59 for Co, *m*/*z* 139 for La and *m*/*z* 232 for Th by the continuous ablation of a reference glass sample, SRM NIST 612. The plasma conditions for the frozen tissue samples (liver) were optimized using the *m*/*z* 68 for Zn (Table I). It is mentioned whenever conditions have been altered to suit individual experiments.

[1]

Auxiliary flow	0.67 L min^{-1}
Carrier gas (Ar) flow	1.12 L min^{-1}
Integration time	1 second
Measured masses	^{12}C, ^{63}Cu, ^{65}Cu, ^{64}Zn, ^{66}Zn, and ^{68}Zn
Internal standard	^{12}C
Laser ablation parameters	*LS × 200 Plus, CETAC*
Laser	Nd: YAG
Wavelength	266 nm
Laser energy	6.5 mJ (100%)
Focus	Sample surface
Fire frequency	10 Hz
Spot size	25–200 μm
Cryo cell temperature	– 80°C

FIG. 2. Laser ablation with cryogenically cooled ablation system.

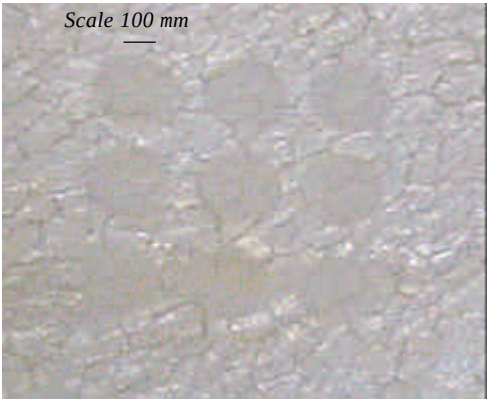

FIG. 3. 3×3 Raster points on NZ lamb liver section (30 *m*m) showing lobular bodies. Laser parameters were 1 burst, 200 *m*m spot size, 6.5 mJ.

3.2. *Samples and standards*

Commercially available lamb's liver and kidney from New Zealand, and Scottish pig kidney were used. In addition, the kidneys of seaweed-eating sheep that live wild on the shore of North Ronaldsay, the most northern island of Orkney, Scotland, were analyzed. Frozen samples were carefully sliced (to about 1 mm thickness) with a scalpel. It is essential to produce a flat surface for the entire tissue in order to reproduce the same ablation conditions for the entire tissue. The use of a microtome would improve the sample preparation.

Standard reference material SRM NIST 612 was used only for tuning, whilst the CRM pig liver (LGC 7112) was used for method validation. The latter is a homogenized paste and contains water. The CRM was pressed between two pieces of glass with a 2-mm spacer and then frozen to generate a dense, tissue-like sample with a smooth surface. To the author's knowledge that is the only commercial CRM that approximates a frozen tissue sample.

3.3. *Calibration method*

Aliquots (0.5 g) of the tissue samples were removed and digested using 5 ml HNO_3 and 2 ml H_2O_2. Digestion was carried out in sealed Teflon bombs using CEM MDS-81 microwave oven. The concentrations were measuring used ICP-AES (Ultratrace Jobin Yvon) and ICP-MS (Spectromass 2000). These tissue samples were also analyzed by the optimized LA-ICP-TOF-MS method. In order to correct for any variation in the ablated material due to laser energy fluctuation, surface roughness or even change of absorption coefficient of the ablated material, the use of carbon (m/z 13/12) as an internal standard was studied. The measured concentrations in the bulk were used to calibrate this method using the ratio of the peak height of analyte and internal standard $^{13/12}$C. Afterwards this calibration was validated by analyzing the standard reference material CRM LGC 7112.

3.4. *Optimization experiments*

The reproducibility of the LA-ICP-TOF-MS system over 5 min ablation was tested by ablating the glass SRM (NIST 612) using 1.02 s integration time, 6.5 mJ power, a spot size of 100 *m*m and a scanning rate of about 10 *m*m/s with a frequency of 20 Hz. At a concentration of about 40 mg/kg, copper and lead gave RSD (relative standard deviation) of approximately 2.5 to 3.5%. In the following section the major ablation and detection parameters were studied using a liver sample and, if not mentioned otherwise, the conditions of Table I apply.

Frozen liver tissue from NZ lamb was sliced to 1 mm and used for laser ablation. Different laser parameters were given to look for efficient ablation processes. Localization of trace elements for mapping was carried out using a cryotome –25°C and a thin tissue section. A small portion of the NZ lamb liver was positioned on to the cryotome block holder and sectioned to get a 30 *m*m thick slice. It was affixed to a clean glass slide and airdried for a few minutes and introduced into the ablation chamber and the image of the liver section was captured on to the screen with the help of a CCD camera fitted to the laser system (Fig. 3).

4. Results and discussion

4.1. *Variation of ablation cell temperature*

In the first experiment, the influence of the cell temperature on the signal stability was tested. Zinc was identified as being the most homogeneous element in the tissue samples. In addition, molybdenum and carbon (internal standard) were measured. Due to the lack of homogeneity a raster of 15 spots (200 *m*m) at 300 *m*m centers was used to identify the stability of the signal. For simplicity, peak heights rather than peak area were used for the calculation of the relative standard deviation (Table II).

The variation of the cell temperature shows the benefit of using a low temperature when tissue samples are ablated. The three selected elements show the same trend; large variation at –20°C, while below –60°C the reproducibility is similar to that achieved when the glass SRM was measured under normal LA conditions.

In our opinion it is necessary to set the ablation cell temperature to at least –60°C. However, it is beneficial to have a safety margin especially if the sample is going to be mapped, which may result in localized heating. Therefore, the temperature of the cell was set to –80°C for the remainder of the study.

Table II
Reproducibility of the signal
Influence of the ablation cell temperature on the reproducibility of the laser signal using a lamb's liver sample (*n* = 15, LA conditions: 100% power, 20 Hz, 200 *m*m spot size, 50 shot).

Isotopes	–20°C	–40°C	–60°C	–80°C
^{13}C	18.2%	10.9%	5.8%	4.1%
^{68}Zn	4.2%	3.8%	2.6%	2.6%
^{98}Mo	22.5%	9.8%	6.4%	6.5%

There is no merit in going to a lower temperature as the o-ring becomes very rigid and does not seal properly. This leads to poor transport of the ablated sample to the plasma. It should be noted here that while the signal intensity varied with the temperature, it was not consistent between elements. This may be due to the generation of extensive water vapour at higher temperature, which may result in a shift of the ionization zone because the plasma turned from dry to wet plasma conditions.

4.2 *Variation of the spot size*

The variation of spot size has a direct influence on the amount of ablated material and on the resolution if a raster grid or a line scan is performed. Since the energy density of the laser remains constant it can be expected that the spot size is directly related to the intensity; this is indeed the case for our samples. Figure 4 shows the signal of zinc with an approximate concentration of about 40 mg/kg fresh weights. At this concentration, a spot size of 10 *m*m just shows the occurrence of a detectable signal and is of little use if the distribution of the element in the tissue is the focus of the investigation. The size used therefore depends on the concentration of the element of interest and the achievable resolution if a tissue is going to be mapped.

A very important point to bear in mind is that the plasma conditions may change significantly if substantial amounts of material are transported into the plasma. This would result in a reduction of the ionization efficiency. However, in these experiments the ablated area does correlate linearly to the intensity of the peaks ($R^2 = 0.9955$). This is very important if the instrument is to be calibrated using the single standard method: the spot size can be varied and the same calibration curve can be used after calculating the amount of material ablated.

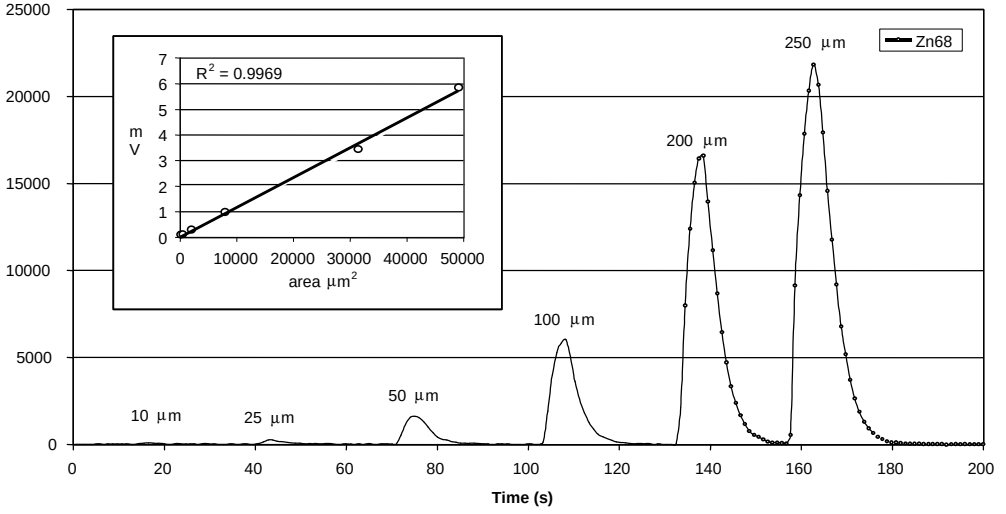

FIG. 4. Variation of raster spots size to intensity of signal *m*/*z* 68 ablated temperature –80°C, 50 shots at 10 Hz with 200 *m*m spot size.

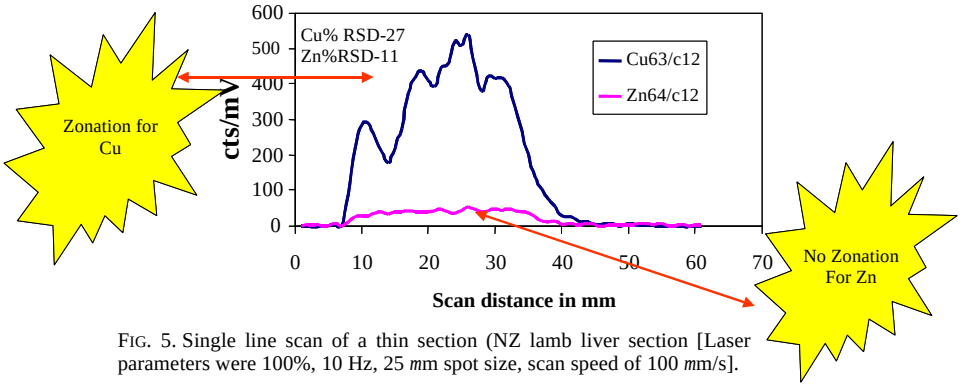

FIG. 5. Single line scan of a thin section (NZ lamb liver section [Laser parameters were 100%, 10 Hz, 25 *m*m spot size, scan speed of 100 *m*m/s].

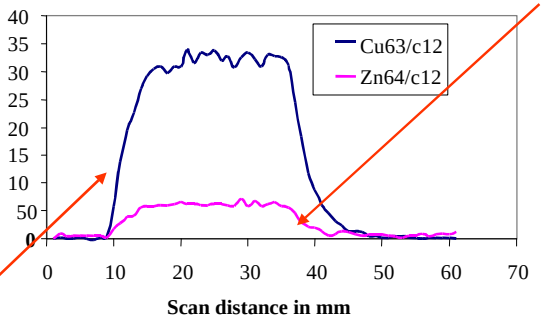

FIG. 6. Single line scan of a homogenized tissue CRM LG7112 pig liver paste [Laser parameters were 100%, 10 Hz, 2.5 *m*m spot size, scan speed of 100 *m*m/s].

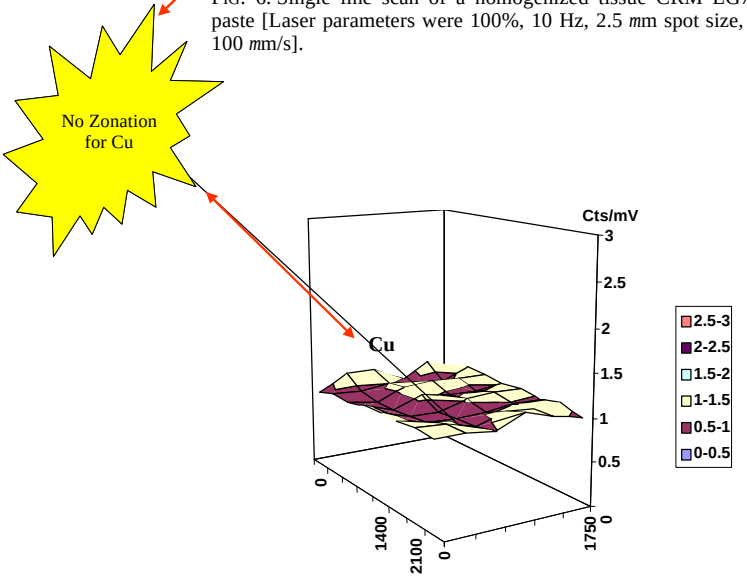

Copper distribution in CRM LG 7112

FIG. 7. Raster scan of homogenized CRM pig liver paste (LG7112) 10 Hz 7×6 rasters, 200 *m*m spot size, 5 bursts.

4.3. *Validation of the calibration method*

Tissue for which the total analysis had been done was analyzed using the laser ablation technique and the following conditions: –80°C, 100% power (~ 6.5 mJ), 10 Hz, 50 shots and 200 *m*m spot.

The selected tissues show quite a variety of element concentration, except for Mo and Zn, which seemed to be very constant. For Cd and Cu, the calibration curves show a good linearity over more than one order of magnitude, although the concentration of the samples is not ideally distributed on this scale and therefore a bit of variation can be expected. The validation using the CRM pig liver is very encouraging. The good accuracy demonstrates that bulk analysis is possible if just one spot is used for the analysis. On the other hand, since accuracy on one spot is acceptable, mapping of a tissue using raster grids should become possible. Using the internal standardization with ^{13}C shows that it is possible to use a one-point calibration curve for the quantification of trace elements in fresh soft tissues. However, care has to be taken for those elements that are not homogeneously distributed. The strategy for bulk analysis is therefore strongly dependent on the distribution pattern of elements.

The detection limits are element-dependent but 0.1 mg/kg lead in the LGC 7112 is clearly detectable if 200 *m*m, 10 Hz and 6.5 mJ power is used. The indicative detection limit is 0.002 mg/kg. For Cd, 0.25 mg/kg in the LGC 7112, the calculated limit of detection based on $3s$ for the blank (when no ablation is taking place) is 0.015 mg/kg (Table III).

5. Mapping of the tissue

In order to see how the different trace elements are distributed in the tissues it is necessary to either raster a grid or to scan a line on the surface. A homogeneous sample (CRM pig liver) was scanned with 25 *m*m spot size and a scanning rate of 100 *m*m/s. Figure 6 shows

Table III
Validation of the method (Accuracy)
Results of calibration function using four different fresh soft tissue samples and its validation with CRM pig liver (LGC 7112); five spots of 200 *m*m

Tissue	[Cd] mg/kg	[Cu] mg/kg	[Zn] mg/kg	[Mo] mg/kg
NZ lamb liver	0.063	6.87	42.4	1.25
Nz lamb kidney	0.094	102.0	39.9	1.89
Pig kidney	0.822	8.21	21.4	0.97
NR sheep kidney	16.9	5.19	39.3	0.44
Slope[¥]	217.73* cts	0.5993* mV	0.4825* mV	1318.8* cts
R^2	0.999	0.986	0.998	0.993
CRM pig liver (LGC 7112) (measured	0.31 ± 0.02	101 ± 6	43.0 ± 1.7	1.8 ± 0.1
Certified	025 ± 0.04	117 ± 8	43.0 ± 2.7	~1#
Detection limits*	0.015	0.05	0.02	~0.01

[a]Zn and Cu are in mV, lower R^2 reflects degree of homogenity.

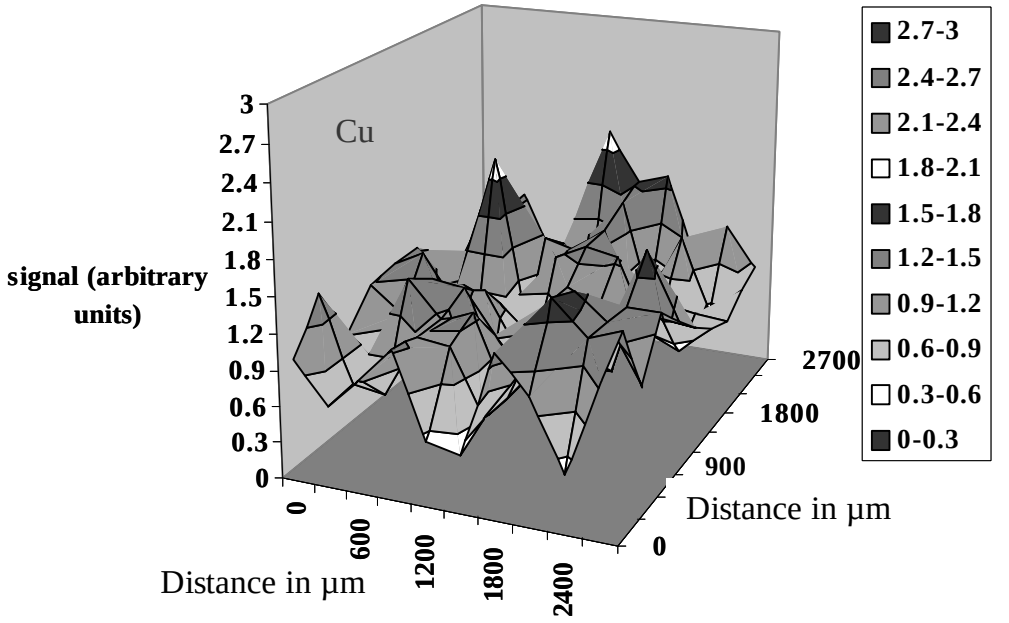

FIG. 8. 10×10 Raster scans of thin NZ lamb liver section shows the zonation of Cu (shown as normalized intensity in arbitrary units).

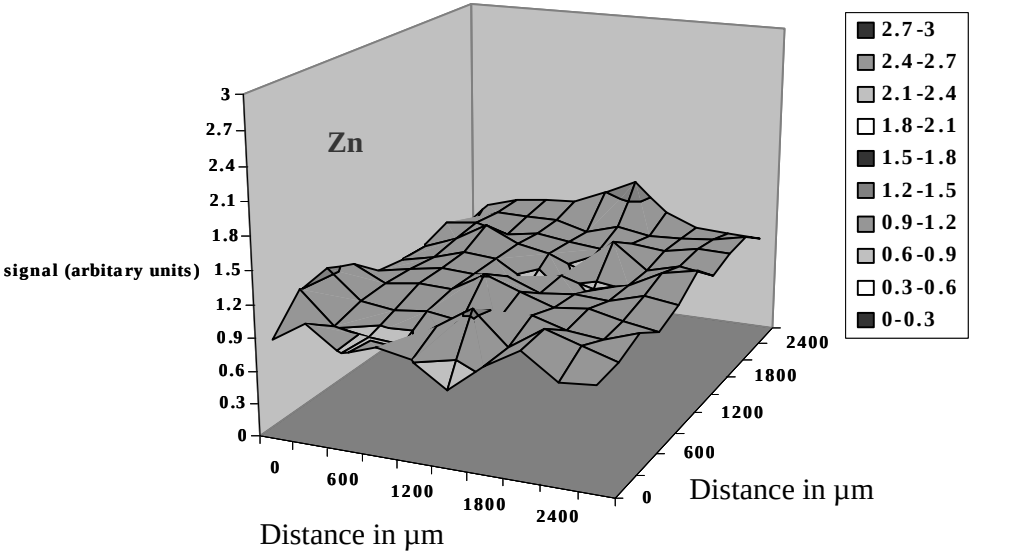

FIG. 9. 10×10 Raster scans of thin NZ liver section showing homogeneous distribution of zinc (shown as normalized intensity in arbitrary units).

the variation of the copper signal on *m*/*z* 63 of a line of about 1.5 mm. The RSD for this signal is about 7.6%. The reproducibility is higher than expected which may point to the heterogeneity or surface roughness of the self-made standard. In order to correct for the variation in the ablation process an internal standard $^{13/12}C$ is used. Using the normalized signal, the reproducibility is improved (RSD 5.3%). This stability is necessary for two-dimensional mapping of frozen soft tissue. One point is significant, the tailing of the copper signal is more pronounced for the $^{63}Cu/^{13}C$ ratio (in contrast to only the ^{63}Cu signal being used). This observation can also be seen in other elements such as Zn, i.e. the RSD for ^{64}Zn is 7.4% but the reproducibility has improved for $^{64}Zn/^{12}C$ (RSD 5.8%). On the contrary, the line scan of NZ lamb liver shows that the RSD of the normalized signal for ^{63}Cu and ^{64}Zn are 27 and 11%, respectively. This means that there are zonations for copper (Fig. 5).

This would mean that the transportation characteristics of organic material are different from the particles that contain the metals. If the sample is completely vaporized, metals would be transported slower than the bulk of the organic material; this is unexpected. The authors do not have any explanation for this observation.

A cryogenically cooled ablation cell enables the direct analysis of thin sections, from fresh soft tissue samples such as liver or kidney, for trace elements using laser ablation ICP-MS. All laser ablation parameters were optimized. A calibration method using three different tissue samples has been validated with CRM pig liver (LGC 7112). Good recoveries (86–124% for certified values) were achieved for Cu (100.9 mg/kg; 117 ± 8 certified), Zn, Cd, Mo using the carbon signal as internal standard (Table III). Therefore this CRM can be used for the quantification of other tissues with similar C-content using a one-point calibration. Detection limits in the lower mg/kg range (Zn: 20 mg/kg) were determined based on 3 sigma of the blank signal with a spatial resolution of less than 200 mm. Figures 6 and 7 explains the homogeneity in copper found in CRM material as compared to the real sam-

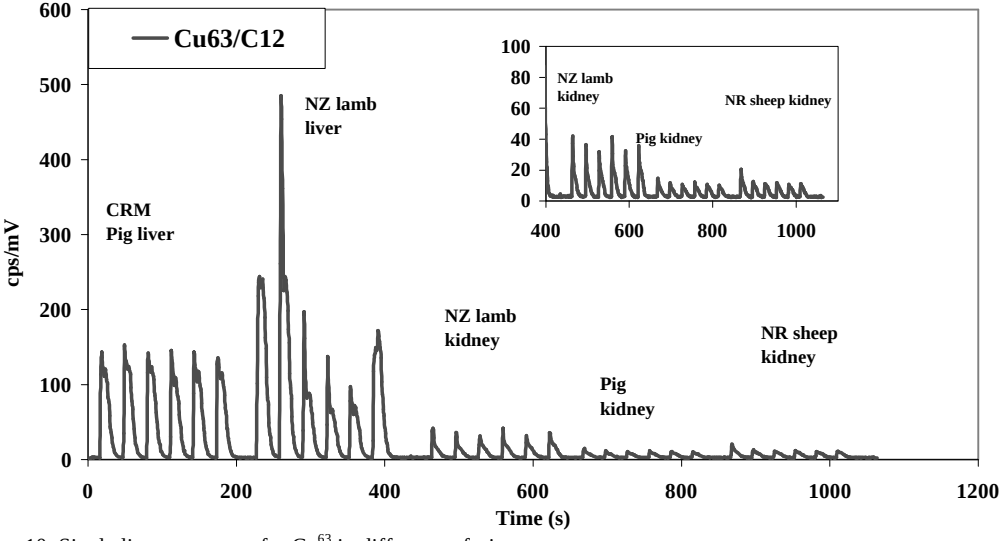

FIG. 10. Single line raster scan for Cu^{63} in different soft tissues.

ple, NZ lamb liver (Fig. 5). On the other hand, zinc shows homogeneity in both CRM and the real sample, NZ lamb liver. The distribution of copper is heterogeneous in NZ lamb liver. Figures 8 and 9 shows the distribution map of copper and zinc in the NZ lamb liver. Figure 10 shows the normalized signal (Cu^{63}/C^{12}) for various tissues.

6. Conclusions

LA coupled to ICP-MS with a cryogenically cooled ablation chamber is the ideal technique for 2D mapping of trace elements in soft tissues. Depending on the concentration of the element present, it may be possible to determine the trace elements directly in tissue samples at a spatial resolution of < 20 *m*m. This technique can be extrapolated to map specific location of the element concern, within an area of 100 *m*m in a microtomic section. LA-ICP-MS is therefore an excellent tool for histologists and molecular cell biologists to correlate certain features in tissues with multi-element distribution of trace elements in the tissues. LA-ICP-TOF-MS has detection limits in the lower *m*g kg^{-1} range. Accuracy is satisfactorily worth using 'C' as internal standard. Precision is good enough to recognise zonations of elements in tissue. Therefore, this technique can be used for various applications like study of metal particle distribution in the lung of workers in occupational exposure, mapping of proteins by overlaying with elemental maps, verification of histopathological conditions caused by metal intoxication, distribution of copper (e.g. in prion diseases) in the hippocampus region of the brain section. Our group is now working towards trace element mapping in the hippocampus region of scrapie-infected mice brain.

References

1. A. Raith, J. Godfey and R. C. Hutton, Quantitative methods using laser ablation ICP-MS evaluation of new glass standards, *Fresenius'. J. Anal. Chem.*, **354**, 789–792 (1996).
2. K. E. Jarvis and J. G. William, Laser ablation inductively coupled plasma mass spectrometry (LA-ICP-MS): a rapid technique for the direct quantitative determination of major, trace and rare earth elements in geological samples, *Chem. Geol.*, **106**, 251–262 (1993).
3. Y. Huang, Y. Shibata and M. Morita, Micro laser ablation inductively coupled plasma mass spectrometry. 1. Instrumentation and performance of micro laser ablation system. *Anal. Chem.*, **65**, 2999–3003 (1993).
4. Andrew M. Dobney, Arjan J. G. Mank, Karl H. Grobecker, Patrick Conneely and Chris G. de Koster, Laser ablation inductively coupled plasma mass spectrometry as a tool for studying heterogeneity within polymers, *Anal. Chim. Acta*, **423**, 9–19 (2000).
5. H. Reinhardt, M. Kriews, H. Miller, O. Schrems, C. Lüdke, E. Hoffmann and J. Skole, Laser ablation inductively coupled plasma mass spectrometry: a new tool for trace element analysis in ice cores, *Fresenius' J. Anal. Chem.*, **370**, 629–636 (2001).
6. Garbe-Schönberg, C. Reimann and V. A. Pavlov, Laser ablation ICP-MS analyses of tree-ring profiles in pine and birch from N Norway and NW Russia–a reliable record of the pollution history of the area, *Environ. Geol.*, **32**, 9–16 (1997).
7. Shaun A. Watmough, Thomas C. Hutchinson and R. Douglas Evans, Development of solid calibration standards for trace elemental analyses of tree rings by laser ablation inductively coupled plasma–mass spectrometry, *Environ. Sci. Technol.*, **32**, 2185–2190 (1998).
8. E. Hoffmann, C. Ludke, H. Scholze and H. Stephanowitz, Analytical investigations of tree rings by laser ablation ICP-MS, *Fresenius'. J. Anal. Chem.*, **350**, 253–259 (1994).
9. S. A. Watmough, T. C. Hutchinson and R. D. Evans, The quantitative analysis of sugar maple tree rings by laser ablation in conjuction with ICP-MS, *J. Environ. Qual.*, **27**, 1087–1094 (1998).

10. U. Narewski, G. Werner, H. Schulz and C. Vogt, Application of laser ablation inductively coupled mass spectrometry (LA-ICP-MS) for the determination of major, minor, and trace elements in bark samples, *Fresenius'. J. Anal. Chem.*, **366**, 167–170 (2000).
11. K. M. Lee, J. Appleton, M. Cooke, F. Keenan and K. Sawicka-Kapusta, Use of laser ablation inductively coupled plasma mass spectrometry to provide element versus time profiles in teeth, *Anal. Chim. Acta*, **395**, 179–185 (1999).
12. Frederika Lochner, John Appleton, Fergus Keenan and Michael Cooke, Multi-element profiling of human deciduous teeth by laser ablation-inductively coupled plasma-mass spectrometry, *Anal. Chim. Acta*, **401**, 299–306 (1999).
13. E. Hoffmann, C. Lüdke, J. Skole, and H. Stephanowitz, E. Ullrich, and D. Colditz, Spatial determination of elements in green leaves of oak trees (*Quercus robur*) by laser ablation-ICP-MS, *Fresenius J. Anal. Chem.*, **367**, 579–585 (2000).
14. G. D. Price and N. J. G. Pearce, Biomonitoring of pollution by *Cerastoderma edule* from the British Isles: a laser ablation ICP-MS study, *Mar. Pollution Bull.*, **34**, 1025–1031 (1997).
15. V. R. Bellotto and N. Miekeley, Improvements in calibration procedures for the quantitative determination of trace elements in carbonate material (mussel shells) by laser ablation ICP-MS, *Fresenius' J. Anal. Chem.*, **367**, 635–640 (2000).
16. Harry Toland, Bill Perkins, Nick Pearce, Fergus Keenan and Melanie J. Leng, A study of sclerochronology by laser ablation ICP-MS, *J. Anal. Atom. Spectrom.*, **15**, 1143–1148 (2000).
17. C. A. Richardson, S. R. N. Chenery and J. M. Cook, Assessing the history of trace metal (Cu, Zn, Pb) contamination in the North Sea through laser ablation-ICP-MS of horse mussel, *Mar. Ecol. Prog. Ser.*, **211**, 157–167 (2001).
18. F. Watt, Nuclear microscope analysis in Alzheimer's and Parkinson's disease: a review, *Cell. Mol. Biol.*, **42**, 17–26 (1996).
19. I. C. Fuentealba, S. Haywood and J. Trafford, Evaluation of histochemical methods for the detection of copper overload in rat liver, *Liver*, **7**, 277–282 (1987).
20. J. Mesjasz-Przybylowicz and W. J. Przybylowicz, Micro-PIXE in plant sciences: present status and perspectives, *Nucl. Instrum. Methods Phys. Res. B*, **189**, 470–481 (2002).
21. P. J. Todd, T. G. Schaaf, P. Chaurand and R. M. Caprioli, Organic ion imaging of biological tissue with secondary ion mass spectrometry and matrix-assisted laser desorption/ionization, *J. Mass Spectro.*, **36**, 355–369 (2001).
22. S. Chandra and G. H. Morrsion, Imaging ion and molecular transport at subcellular resolution by secondary ion mass spectrometry, *Int. J. Mass Spectro. Ion Processes*, **143**, 161–176 (1995).
23. T. C. Iancu, D. P. Perl, I. Sternlieb, E. Leshinsky, E. H. Kolodny and A. Hsu, The application of laser microprobe mass analysis to the study of biological material, *Biometals*, **9**, 57–65 (1996).
24. H. Kupper, E. Lombi, F. J. Zhao, G. Wieshammer and S. P. McGrath, Cellular compartmentation of nickel in the hyperaccumulators *Alyssum lesbiacum*, *Alyssum bertolonii* and *Thlaspi goesingense*, *J. Expl. Bot.*, **52**, 2291–2300 (2001).
25. H. O. Ylanen, C. Ekholm, N. Beliaev, K. H. Karlsson and H. T. Aro, Comparison of three methods in evaluation of bone ingrowth into porous bioactive glass and titanium implants, *Key Engng Mat.*, **192**, 613–616 (2000).
26. J. A. Centeno and F. B. Johnson, Microscopic identification of silicone in human breast tissues by infrared microspectroscopy and X-ray microanalysis, *Appl. Spectrosc.*, **47**, 341–345 (1993).
27. V. Mizuhira, H. Hasegawa and M. Notoya, Microwave fixation and localization of calcium in synaptic terminals and muscular cells by electron probe X-ray microanalysis and electron energy-loss spectroscopy imaging, *Acta Histochem. Cytochem.*, **30**, 277–301 (1997).
28. P. Chaurand and R. M. Caprioli, Direct profiling and imaging of peptides and proteins from mammalian cells and tissue sections by mass spectrometry, *Electrophoresis*, **23**, 3125–3135 (2002).
29. D. Günther, S. E. Jackson and H. P. Longerich, Laser ablation and arc/spark solid sample introduction into inductively coupled plasma mass spectrometers, *Spectrochim. Acta B*, **54**, 381–409 (1999).

Printed and published by Dr S. Venkadesan, Executive Editor, *Journal of the Indian Institute of*